JLB 12 (2026) 100471

Contents lists available at ScienceDirect

The Journal of Liquid Biopsy

journal homepage: www.sciencedirect.com/journal/the-journal-of-liquid-biopsy

Exploring tear biomarkers with shotgun proteomics for retinoblastoma diagnosis: a pilot study

Andrés Rodríguez-Rodríguez [a], Karla Grisel Calderón-González [a], Juan Pedro Luna-Arias [b], Mariana Moctezuma-Dávila [c], Martha Rangel-Charqueño [d], Bernardo Yañez-Soto [e], Vanesa Olivares-Illana [a,*], Jesús Hernández-Monge [f,**]

[a] Laboratorio de Interacciones Biomoleculares y Cáncer, Instituto de Física, Universidad Autónoma de San Luis Potosí, Mexico
[b] Departamento de Biología Celular, Centro de Investigación y de Estudios Avanzados del Instituto Politécnico Nacional (Cinvestav-IPN), Av. Instituto Politécnico Nacional 2508, Col. San Pedro Zacatenco, Gustavo A. Madero, C.P. 07360, Ciudad de México, Mexico
[c] Ophthalmic pathology Fellow at Houston Methodist Hospital, USA
[d] Departamento de Oftalmología, Hospital Central "Ignacio Morones Prieto", San Luis Potosí, Mexico
[e] Investigador por México SECIHTI– Laboratorio de Biomarcadores Moleculares, Instituto de Física, Universidad Autónoma de San Luis Potosí, Mexico
[f] Investigador por México SECIHTI– Instituto de Física, Universidad Autónoma de San Luis Potosí, Mexico

ARTICLE INFO

Keywords:
Retinoblastoma
Biomarkers
Tears
Proteome

ABSTRACT

The most common ocular neoplasia among children is retinoblastoma. Currently, the diagnosis of this disease is essentially clinical, taking a biopsy is contraindicated owing to the high risk of causing metastasis. Therefore, it is imperative the development of a method to diagnose this disease through a non-invasive fashion. We choose tears as they fulfill the former precept. Through proteomic analysis we observed 52 up regulated and 48 down regulated proteins among retinoblastoma cases as compared to healthy children. Among these proteins, we identified several previously associated with retinoblastoma such as apolipoprotein A-1 (*APOA1*). We confirmed up regulation of *APOA1* and S100 binding calcium A9 (*S100A9*) which revealed faithful concordance to the predicted values from mass spectrometry.

1. Introduction

Retinoblastoma (RB) is the most common intraocular cancer among children. The incidence of RB is 1 case for every 15,000 to 20,000 live births and 9000 new cases are estimated per year around the world [1]. Interestingly, the annual report of cancer in U.S., showed that the Latin population resulted in higher incidence of retinoblastoma as compared to non-Latin population [2]. In Chiapas, one of the poorest states to the south of Mexico, it was reported 21.4 cases of retinoblastoma per million children per year, which is 5 times higher than other states that report an average of 5.4 cases per million children [3]. The early diagnosis of RB is a key obvious factor for bringing the treatment into early stages. The observation of clinical signs such as leukocoria (56% of cases) and strabismus (20%) usually are the best chance of doctors for detection of this disease [4,5]. Therefore, searching for biomarkers hopefully will help in early diagnosis and opportune treatment of this disease. In this regard, we pursue getting close to the identification of potential biomarkers through the use of tears as biological source because of its proximity to the tumor, for its easy way to be obtained overall trough a non-invasive way, and for its probed feasibility as a biomarker source for other ocular and non-ocular diseases [6–11]. In addition, the data obtained inhere will help in understanding the underlying molecular bases of retinoblastoma as well as for possible identification of molecular therapeutic targets.

2. Material and methods

2.1. Sample collection

Tears were obtained from 1 to 5 years old-children healthy or with retinoblastoma from the Central Hospital "Ignacio Morones Prieto", San Luis Potosí, México. The method for tear collection was the Schirmer's

* Corresponding author. Laboratorio de Interacciones Biomoleculares y Cáncer, Instituto de Física, Universidad Autónoma de San Luis Potosí, San Luis Potosí, Mexico.
** Corresponding author. Laboratorio de Biomarcadores Molecualres, Instituto de Física, Universidad Autónoma de San Luis Potosí, San Luis Potosí, Mexico.
E-mail addresses: vanesa@ifisica.uaslp.mx (V. Olivares-Illana), jesus.hernandez@secihti.mx (J. Hernández-Monge).

https://doi.org/10.1016/j.jlb.2026.100471
Received 4 February 2026; Received in revised form 9 April 2026; Accepted 17 April 2026
Available online 22 April 2026

test under the scheme of the Community Eye Health Journal [12].

2.2. Extraction of proteins

The strip was incubated with 100 µL of extraction buffer (ammonium bicarbonate 100 mM, Urea 8M, protease inhibitors (Complete, Roche)) for 1 h at room temperature. The soluble proteins were then precipitated with 6 vol of cold acetone overnight at −20 °C; the pellet was resuspended with 20 µL of TEAB-Urea 8M + protease inhibitors. Every sample was stored at −80 °C. The protein quantification was done by Bicinchoninic Acid Assay (BCA).

2.3. Sample processing and label-free mass spectrometry

The tear proteins of 10 children with retinoblastoma and 10 healthy controls were pooled into two groups, each group was containing 150 µg of total protein. These samples were processed at CINVESTAV-IPN, Mexico City, for the mass spectrometry analysis. Briefly, proteins were enzymatically digested using iST Sample Preparation Kit® (PreOmics, Munich, GER); 50 µL of "Lyse" reagent was added to protein, placed in a heating block during 10 min, 95 °C at 1000 rpm then, samples were sonicated during 20 cycles using BioRuptor Pico® (Diagenode, Liège, BEL) 30 s ON/30 s OFF per cycle. Protein samples were digested using 50 µL of a Lys-C/Trypsin mix ("Digest" reagent) and heating at 37 °C during 2 h. Resulting peptides were cleaned in an iST cartridge using a "Wash 1" buffer to eliminate hydrophobic contaminants and "Wash 2" buffer to eliminate hydrophilic contaminants molecules; afterward, peptides were eluted using "Elute" reagent and subsequently evaporated to dryness in a SpeedVac (TermoFisher Scientific, Waltham, USA), then, peptides were resuspended with "LC-Load" reagent and a aliquot of alcohol dehydrogenase 1 (*ADH1*) from *Saccharomyces cerevisiae* (Uniprot, accession number P00330; 1 pmol μl^{-1}) was added as internal standard to each sample in order to obtain a final concentration of 25 fmol μL^{-1}. Finally, samples were stored at −80 °C until LC-MS analysis.

Quantitative proteomic analysis was performed in a UPLC Nano Acquity M-Class coupled with a QTOF Synapt G2-*Si* (Waters; Milford, MA, USA), according to the method of Ríos-Castro et al., 2020 [13]. Tryptic peptides were separated on an HSS T3 C18 column (Waters, Milford, MA); 75 µm × 150 mm, 100 Å pore size, 1.8 µm particle size; using a mobile phase A, 0.1% formic acid (FA) in H2O, and mobile phase B, 0.1% FA in acetonitrile (ACN) under the following gradient: 0 min 7% B, 121.49 min 40% B, 123.15 to 126.46 min 85% B, 129 to 130 min 7% B, at a flow of 400 nL min^{-1} and 45 °C on column compartment. The spectra data were acquired using data-independent acquisition (Full--Scan DIA) approach through High-Definition Multiplexed MS/MS ($HDMS^E$) mode [14,15]. Parameters on ionization source were set with the following values: 2.75 kV in the capillary emitters, 30 V in the sampling cone, 30 V in the source offset, 70 °C for the source temperature, 0.5 bar for the nanoflow gas and 150 L h^{-1} for the purge gas flow. Low and high energy chromatograms were acquired in positive mode in a range of m/z 50−2000 with a scan time of 500 ms. Precursor ions were fragmented in the transfer cell using a collision energy ramp from 19 to 55 eV. and the sample was injected 3 times for statistical purposes.

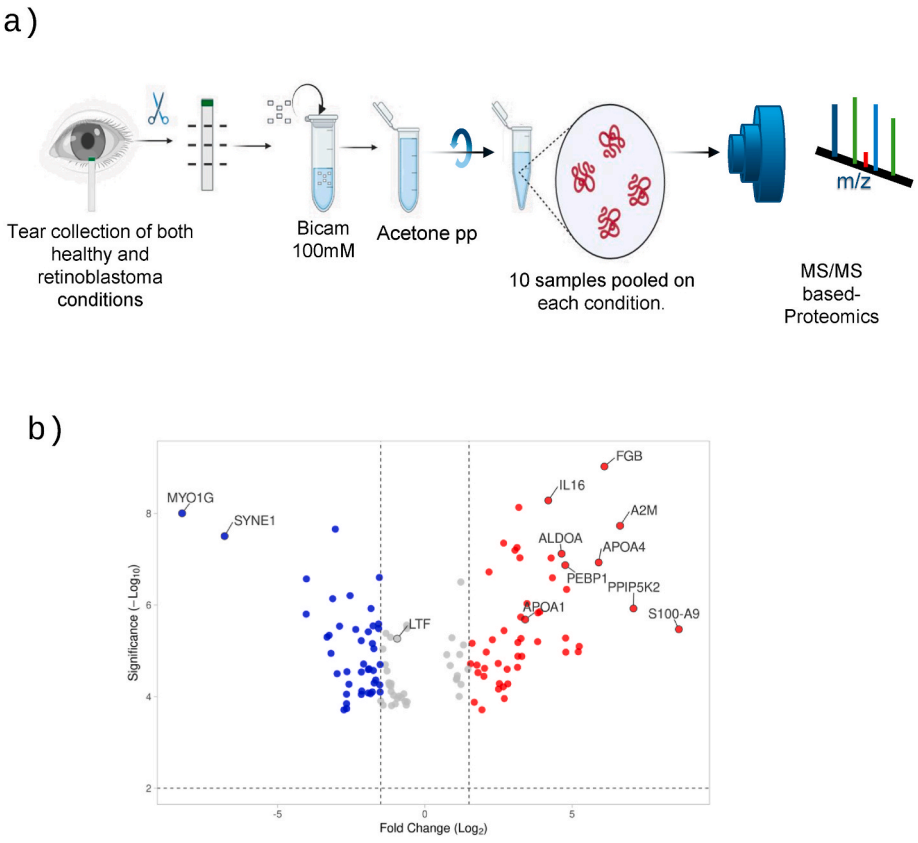

Fig. 1. a) Workflow for tear collection followed by MS/MS based proteomics. Tear collection was done according to Schirmer method; the strip paper is put at the edge of the eyelid, so the tears are absorbed by capillarity. The proteins are solubilized with ammonium bicarbonate solution followed by acetone precipitation. b) Dysregulated proteins in tears of retinoblastoma infants. A volcano plot is shown representing the differential expression of the most statistically significant proteins in retinoblastoma tears. Red circles are up-regulated proteins, blue circles are down-regulated proteins and gray circles represent no change in protein expression. On the x-axis is shown the fold change for each protein (values are represented as Log2 of the ratio retinoblastoma/control); the y-axis indicates significance (values are represented in -log10 of p-value by triplicate experiments).

2.4. MS data analysis

Generated *.raw files were compared and quantified using QI software for proteomics V3.0.3 (Nonlinear Dynamics, Newcastle, UK) based in a target decoy strategy [16,17] against a *Homo sapiens* database (downloaded from UniProt, UP000005640, 81791 protein sequences, plus ADH1, Uniprot accession: P00330). The parameters used for the protein database search were trypsin as cutting enzyme and one missed cleavage; carbamidomethyl (C) as a fixed modification and oxidation (M), amidation (C– terminal), deamidation (Q, N) and phosphorylation (S, T, Y) as variable modifications; default peptide and fragment tolerance and false discovery rate ≤1%; all false positive identifications (Reversed proteins) and proteins with one peptide identified were discarded for subsequent analysis besides, Synapt G2-*Si* was calibrated with [Glu1]-fibrinopeptide, $[M+2H]^{2+} = 785.84261$ at less than 1 ppm across all MS/MS measurements. Quantification of proteins was calculated based on the average MS signal response of the three most intense tryptic peptides (Top3) [18,19] according to the following equations:

$$Top3 = \frac{i1 + i2 + i3}{3}$$

where, *i*1, *i*2, and *i*3 are the spectrometric counts of the most intense peptides.

$$\bigcup SRF = \frac{Top3}{fmol_{ADH1}}$$

USRF is the universal signal response factor and $fmol_{ADH1}$ is the amount (fmol) of ADH1 injected into the LC column.

$$fmol = \frac{Top3_x}{USRF}$$

$Top3_x$ is equal to the top 3 values of each identified protein in the sample.

The ratio was obtained based on the fmol calculated for each characterized protein in retinoblastoma condition by the fmol calculated in the healthy controls. Proteins were considered dysregulated when their proportion was ±1.3 (expressed in logarithm base 2). Retinoblastoma exclusive proteins were also found within our data. Additionally, we calculated the coefficient of variation, this statistical measure tells us the size of a standard deviation in relation to its mean even if the means between groups are drastically different from each other, that is the higher the CV the greater the level of dispersion around the mean, so that values close to 0 are the ideal ones meaning more solid results.

2.5. Data availability

The original data of this study, including identified peptide sequences as well as original intensities (Hi3) used in the label free quantification for each identified protein are available at https://doi.org/10.5061/dryad.x69p8czxq.

2.6. Biostatistical analysis

The proportion of each protein was calculated by dividing the mean of protein abundance from retinoblastoma patients by their corresponding proteins of health individual controls. A logarithm base 2 to fold change (Y-axis) as well as a negative logarithm base 10 (x-axis) to the p-value (≥0.05) was applied to remove skewness and improve visibility of the plot. Some of the identified proteins were excluded as they are quite possibly present because a source of contamination such as keratins. We set a coefficient of variation equal or less than 0.2. The ANOVA test ($P \leq 0.05$) with Bonferroni correction was performed.

2.7. Bioinformatic platforms

The functional enrichment was performed through the Protein ANalysis THrough Evolutionary Relationships (PANTHER) classification system (https://www.pantherdb.org/). We chose by default the molecular functional annotation classification to achieve the first panoramic view. We used the STRING database [20] (https://string-db.org/) to analyze functional enrichment of Interacting proteins alongside the Cytoscape software, Version 3.10.2.

2.8. Western blotting

Equal tear protein amounts of both health and disease condition were loaded and resolved in 8% or 15% SDS-PAGE. The gels were transferred on BioTrace NT pure nitrocellulose blotting membrane (PALL Corporation) and blocked with 5% non-fat dry milk in PBS pH 7.6 containing 0.1% Tween-20. Proteins were then probed with corresponding antibodies; anti-APOA1 (1:500, Cat# PA520721), anti-S100A9 (1:500 Cat#MA517624), and anti-Lacto transferrin (1:500, PA5-95513) from Invitrogen; all antibodies probed worked in 5% non-fat dry milk in PBS pH 7.6.

3. Results

3.1. Tear proteins collection and identification by MS/MS

Because taking a biopsy from retinoblastoma implies a very high risk to provoke metastasis, we believe it is mandatory to develop a non-invasive method to assess or diagnose this disease. Herein, we show a study where a total of 10 retinoblastoma patients versus 10 healthy controls were pooled and compared for identification of differential tear

Table 1
List of proteins up-regulated (red box) and down-regulated (green box) in patients with retinoblastoma as compared with healthy children.

Accession #	Description	Peptide count	Unique peptides	Confidence score	Mass
P06702	Protein S100-A9	45	37	190.2236	13299.061
O43314	Inositol hexakisphosphate and diphosphoinositol-pentakisphosphate kinase 2	4	1	17.9549	141661.5445

P01023	Alpha-2-macroglobulin	80	65	483.9773	164716.9032
P02675	Fibrinogen beta chain	30	27	150.4349	56612.6167
P06727	Apolipoprotein A-IV	13	9	78.2385	45372.0928
P01859	Immunoglobulin heavy constant gamma 2	11	4	63.573	36527.9778
Q99758	Phospholipid-transporting ATPase ABCA3	4	1	17.3319	192959.2976
P32119	Peroxiredoxin-2	8	7	39.1489	22063.0168
P01860	Immunoglobulin heavy constant gamma 3	14	1	118.9545	42313.4888
Q12767	Transmembrane protein 94	6	3	44.5593	153717.4415
P30086	Phosphatidylethanolamine-binding protein 1	4	3	27.1099	21170.8601
P04075	Fructose-bisphosphate aldolase A	7	6	31.2572	39876.2787
O75533	Splicing factor 3B subunit 1	4	2	27.0226	146572.0183
O75581	Low-density lipoprotein receptor-related protein 6	5	2	24.0144	183452.0657
Q14005	Pro-interleukin-16	4	2	16.6349	143064.1528
P02765	Alpha-2-HS-glycoprotein	5	4	13.4565	40139.1565
P00558	Phosphoglycerate kinase 1	9	8	60.7298	45013.9805
P01009	Alpha-1-antitrypsin	57	51	276.1896	46907.7136
P11021	78 kDa glucose-regulated protein	8	5	63.5379	68206.177
P02647	Apolipoprotein A-I	54	47	234.6315	30777.8694
P07737	Profilin-1	14	13	54.9807	15225.3488
P31150	Rab GDP dissociation inhibitor alpha	2	2	8.5014	51210.1274

P63261	Actin_ cytoplasmic 2	30	13	234.8121	42135.1246
Q38SD2	Leucine-rich repeat serine/threonine-protein kinase 1	14	3	66.8246	228529.7019
P08603	Complement factor H	8	5	45.2973	143772.7447
P23528	Cofilin-1	7	7	43.8853	18730.6344
Q9UDR5	Alpha-aminoadipic semialdehyde synthase_ mitochondrial	3	2	12.1027	102873.3602
P63104	14-3-3 protein zeta/delta	10	5	78.7958	27916.2394
Q7L576	Cytoplasmic FMR1-interacting protein 1	6	2	31.1469	146836.5092
O43151	Methylcytosine dioxygenase TET3	5	4	23.1469	195928.7812
Q9UHG3	Prenylcysteine oxidase 1	3	2	13.9374	57039.4505
P68133	Actin_ alpha skeletal muscle	26	13	163.2121	42393.3153
Q8TEW0	Partitioning defective 3 homolog	7	4	25.8899	151936.5958
O75334	Liprin-alpha-2	3	1	12.1734	143804.1226
P02768	Albumin	156	124	495.1103	71362.7109
P05109	Protein S100-A8	27	24	113.9828	10891.5551
Q9BQS8	FYVE and coiled-coil domain-containing protein 1	4	2	16.5034	168693.6707
Q562R1	Beta-actin-like protein 2	9	1	58.7607	42345.4528
Q92833	Protein Jumonji	2	1	7.5749	140388.4602
Q12756	Kinesin-like protein KIF1A	13	4	62.4941	192661.2248
Q5BJF6	Outer dense fiber protein 2	5	3	22.5766	96199.8579
Q86UP2	Kinectin	4	3	18.6023	156560.6404

P04406	Glyceraldehyde-3-phosphate dehydrogenase	14	10	80.998	36224.3681
P14618	Pyruvate kinase PKM	21	15	133.7239	58507.2826
P08185	Corticosteroid-binding globulin	3	3	21.6574	45312.064
Q14156	Protein EFR3 homolog A	4	2	17.4148	97043.579
P25815	Protein S100-P	3	3	20.7876	10456.9572
P04004	Vitronectin	4	4	19.4676	55104.0374
Q15643	Thyroid receptor-interacting protein 11	8	1	38.3062	228271.0222
P62937	Peptidyl-prolyl cis-trans isomerase A	14	12	75.0691	18240.6427
P13569	Cystic fibrosis transmembrane conductance regulator	4	1	16.3537	169168.3623
P09211	Glutathione S-transferase P	18	12	120.5637	23583.9696
P61626	Lysozyme C	85	73	213.2954	16993.2636
Q15020	Squamous cell carcinoma antigen recognized by T-cells 3	4	2	18.4972	112813.3069
O60296	Trafficking kinesin-binding protein 2	4	2	17.1726	102331.6495
Q96JM4	Leucine-rich repeat and IQ domain-containing protein 1	8	4	38.1738	201410.6189
O75140	GATOR complex protein DEPDC5 (Fragment)	3	1	17.0995	90430.121
Q08380	Galectin-3-binding protein	12	9	66.7111	66243.5215
Q8WXW3	Progesterone-induced-blocking factor 1	4	3	18.3117	90089.9264
O43520	Phospholipid-transporting ATPase IC	6	2	28.6109	144893.2284
Q9NY65	Tubulin alpha chain	3	1	20.5013	48034.4162

Q5H8C1	FRAS1-related extracellular matrix protein 1	6	3	19.4383	245979.5421
Q9UGL1	Lysine-specific demethylase 5B	6	2	23.1522	178794.314
Q5GLZ8	Probable E3 ubiquitin-protein ligase HERC4	3	1	21.0211	119988.747
Q86VS8	Protein Hook homolog 3	3	2	7.8532	83525.1807
P81274	G-protein-signaling modulator 2	3	2	19.8907	79052.4639
Q6NZI2	Caveolae-associated protein 1	4	2	14.2325	43476.19
P12273	Prolactin-inducible protein	46	36	111.1591	16857.6295
O95831	Apoptosis-inducing factor 1_ mitochondrial	2	2	7.9274	67185.8463
O14646	Chromodomain-helicase-DNA-binding protein 1	7	4	24.1467	197828.3201
Q3V6T2	Girdin	24	9	140.9834	185935.9803
Q9P2F5	Storkhead-box protein 2	7	5	33.41	103811.9611
O95996	Adenomatous polyposis coli protein 2	2	1	8.1413	246115.9464
A6NHC0	Calpain-8	4	2	12.7893	80171.0646
P23229	Integrin alpha-6	15	7	64.2295	127803.2208
Q5TB80	Centrosomal protein of 162 kDa	10	4	47.8044	162456.5274
O15297	Protein phosphatase 1D	2	2	7.5888	67416.5952
Q5TB30	DEP domain-containing protein 1A	4	3	14.2051	93986.2273
O43379	WD repeat-containing protein 62	2	1	10.7147	159658.7743

Q8NEE8	Tetratricopeptide repeat protein 16	3	1	17.5283	99164.4443
A5PLK6	Regulator of G-protein signaling protein-like	3	1	22.2229	126885.9896
P00330	Alcohol dehydrogenase 1	42	36	142.3779	37305.4483
Q8IWJ2	GRIP and coiled-coil domain-containing protein 2	31	12	133.9206	196993.4358
P07384	Calpain-1 catalytic subunit	6	4	31.2414	82517.4807
Q9BYT9	Anoctamin	3	1	11.7376	122684.9184
Q9NX02	NACHT_ LRR and PYD domains-containing protein 2 (Fragment)	2	1	8.0414	101545.2605
Q8NEN0	Armadillo repeat-containing protein 2	6	3	30.5933	98121.3229
P09228	Cystatin-SA	4	2	37.7231	16729.8505
O95163	Elongator complex protein 1	6	3	30.4757	151908.3026
P37088	Amiloride-sensitive sodium channel subunit alpha	6	1	30.8518	76901.4085
Q9BTW9	Tubulin-specific chaperone D (Fragment)	2	2	16.6993	56214.2117
O60315	Zinc finger E-box-binding homeobox 2	4	1	28.53	140620.5018
Q9NR96	Toll-like receptor 9	6	1	27.3898	117513.9498
Q92619	Rho GTPase-activating protein 45	5	2	21.2103	125926.1027
O95490	Adhesion G protein-coupled receptor L2	5	4	24.9547	166807.3886
Q6UWY5	Olfactomedin-like protein 1	3	1	20.237	46407.2049
A0A1W2PS85	BIVM-ERCC5 readthrough	2	1	8.7301	159960.4219

P55072	Transitional endoplasmic reticulum ATPase	3	3	18.6446	90006.2895
Q8NF91	Nesprin-1	3	1	11.9475	112640.4417
B0I1T2	Unconventional myosin-Ig	3	2	12.8523	117468.7302

Up- regulated
Down regulated

protein expression through mass spectrometry-based proteomics (Fig. 1a).

This analysis resulted in a total of 1035 proteins being identified. From these, 188 proteins were filtered as follows: 52 overexpressed and 48 sub expressed in children with retinoblastoma as compared to health controls, and 77 proteins were only present in the retinoblastoma condition but not in health group. The proteins found up-regulated and down-regulated (dysregulated proteins) are visualized in the volcano plot according to statistical significance and fold change (Fig. 1b). The list of both up and down regulated proteins is depicted in Table 1, as well as those proteins present only in retinoblastoma cases in Table 2.

3.2. Functional enrichment of proteins

For the comprehensive organization of proteomic information we used the Protein ANalysis THrough Evolutionary Relationships (PANTHER) classification system (https://www.pantherdb.org/).

The PANTHER classification analysis was done according to molecular function annotation parameter. The dysregulated proteins in retinoblastoma were arranged in two main groups, the binding (40%) and catalytic (24%) function (supplementary Fig. 1 a-I and 1 a-II).

Within the binding function classification, we found remarkably interesting proteins. For instance, we observed the cytoskeleton remodeling proteins Cofilin-1 and profilin-1 upregulated (supplementary figure 1 g), which have direct repercussion on metastasis [21]. Profilin1 was associated with tumor infiltration, lymph node metastasis, and tumor-node-metastases (TNM) in gastric cancer. Accordingly, silencing profilin inhibited invasion and migration of gastric cancer cells [22].

In turn, within the proteins that carry out the catalytic task (supplementary Fig. 1 c-I), Kinesin-like protein (KIF1A) is up regulated. KIF1A protein stands out because it has been proposed as a potential biomarker for many other types of cancers, such as oral squamous cell carcinomas, breast cancer, nasopharyngeal carcinoma and neuroblastoma [23]. Furthermore, another study showed its orthologue KIF11 upregulated in tumor tissue of retinoblastoma [24]. Among down regulated proteins within the hydrolase activity group (supplementary Fig. 1 c-I), we found the lysozyme protein which is a renowned component of the antibacterial defense in tears, but it has also other interesting roles. In gastric and lung cancer it has antiproliferative effects as well as in breast cancer [25], therefore it makes sense the diminished level of this important protein in retinoblastoma.

Regarding proteins present only in the retinoblastoma condition (supplementary Fig. 1 d-f), the sub-classification of proteins was very similar to the former of dysregulated proteins (supplementary Fig. 1 a-c). The most remarkable change is the appearance of a new group: molecular adaptor activity. Within this last group appears the Histone acetyl transferase KAT6B, whose inhibition with small molecules in breast cancer goes in trial phase 1 [26]. It was also interesting the presence of Threonine-tRNA ligase 2 (TARS2) and the Asparagine synthetase within ligase activity group (Supplementary figure 1 e). Both enzymes are linked to regulation of mTOR activity, a key pathway in cellular growth, protein synthesis, autophagia, cellular metabolism, among other processes [27,28].

3.3. Protein interactome

We wanted to explore the interacting proteins, using the same classification as in the PANTHER platform. Accordingly, setting molecular function classification, the STRING and Cytoscape tools showed 5 most significant activities, namely protein binding, small molecule binding, antioxidant activity, endopeptidase inhibitor activity and cell adhesion molecule binding (Supplementary Fig. 2). It Is worth to highlight that several members of the s100 family are present within these networks such as S100A8, S100A9 and S100P, all of them overexpressed in retinoblastoma. The first two form a heterodimer that has been involved in multiple signaling pathways promoting tumor development, growth and metastasis by interfering with metabolism and microenvironment [29]. On the other hand, S100P has also similar activities. It has been found also up regulated in cancer cell lines of breast, pancreas and ovary carcinomas and it has been proposed as a potential diagnostic biomarker as well [30,31].

Interestingly, when we submitted the data of proteins present only in the retinoblastoma condition, the cytoscape software did not show any network under the molecular function classification. Instead, the top significant categories were abnormality of the eye and abnormality of the nervous system, which makes perfect sense with the class of data we were using (Fig. 2). Very Interesting proteins can be highlighted from these interacting networks. In Fig. 2 a, a predicted association can be observed between Budding Uninhibited by Benzimidazoles 1 (BUB1B) and KIF20A. BUB1B is a serine/threonine-protein kinase that functions as a mitotic checkpoint by regulating the assembly of the mitotic spindle. Silencing of BUB1B inhibited the JNK/c-Jun signaling pathway that increased the expression of proapoptotic proteins and decreased the expression of anti-apoptotic proteins in colorectal cancer cells [32]. In turn, KIF20A has multiple roles in promotion of cancer such as invasion and metastasis through enhancing of Golgi secretion of Matrix Metalloprotease-2 (MMP2) and MMP9, drug resistance and proliferation [33,34]. The association BUB1 and KIF20A, resembles the positive feedback between KIF4A and BUB1, since the silencing of KIF4A led to downregulation of BUB1 and consequent suppression of cell proliferation [35]. It can also be seen in Fig. 2 a, that through KIF20A other members of the Kinesin superfamily of proteins are Interacting such as KIF16B and KIF13B; KIF13B is essential for the trafficking of Vascular

Table 2
List of proteins identified only in children with retinoblastoma.

Accession #	Description	Peptide count	Unique peptides	Confidence score	Mass
Q8N3Y1	F-box/WD repeat-containing protein 8	4	1	21.2837	67907.2135
Q9Y263	Phospholipase A-2-activating protein	2	1	15.3945	88696.938
Q86YS3	Rab11 family-interacting protein 4	4	3	24.3598	72612.6342
P15311	Ezrin	7	1	40.8089	69485.8854
Q12789	General transcription factor 3C polypeptide 1	3	1	11.6265	241213.297
Q9UPT5	Exocyst complex component 7	4	1	20.9437	83781.2242
P24158	Myeloblastin OS=*Homo sapiens*	2	1	11.7669	28263.292
P35913	Rod cGMP-specific 3′_5′-cyclic phosphodiesterase subunit beta	3	1	13.2141	99533.5529
Q13751	Laminin subunit beta-3 OS=*Homo sapiens*	4	1	17.1567	133450.57
Q9Y4D7	Plexin-D1 OS=*Homo sapiens*	5	2	19.4887	215428.927
P47755	F-actin-capping protein subunit alpha-2	2	1	9.6124	33177.2497
Q9UQD0	Sodium channel protein OS=*Homo sapiens*	3	1	18.6716	223009.339
P61158	Actin-like protein 3 OS=*Homo sapiens*	2	1	9.744	42289.1596
Q8IX94	cTAGE family member 4 OS=*Homo sapiens*	3	1	12.4227	88331.2263
K7EQ86	KIAA0100_ isoform CRA_a OS=*Homo sapiens*	4	1	25.5488	239693.329
O94988	Protein FAM13A OS=*Homo sapiens*	6	2	19.1619	117673.116
Q9NZI5	Grainyhead-like protein 1 homolog	2	1	8.3997	70398.4999
Q96L93	Kinesin-like protein KIF16B OS=*Homo sapiens*	4	1	16.8991	152581.815
O14639	Actin-binding LIM protein 1 OS=*Homo sapiens*	2	1	13.4213	89569.577
P53675	Clathrin heavy chain 2 OS=*Homo sapiens*	5	1	19.9291	189140.241
O14647	Chromodomain-helicase-DNA-binding protein 2 OS=*Homo sapiens*	8	2	33.5546	212313.236
Q8N1W1	Rho guanine nucleotide exchange factor 28	3	1	18.6877	194000.876
O43295	SLIT-ROBO Rho GTPase-activating protein 3	6	1	29.2218	125473.503
Q96N46	Tetratricopeptide repeat protein 14	5	1	22.4789	88832.0936
P19827	Inter-alpha-trypsin inhibitor heavy chain H1	7	5	41.4694	101845.516
P04196	Histidine-rich glycoprotein	2	1	11.5251	60547.8329
O60566	Mitotic checkpoint serine/threonine-protein kinase BUB1 beta	2	1	8.0121	120857.029
Q16836	Hydroxyacyl-coenzyme A dehydrogenase_ mitochondrial	3	1	16.0604	34651.939
P42262	Glutamate receptor 2	3	1	11.9805	99448.5652
Q9H410	Kinetochore-associated protein DSN1 homolog (Fragment)	2	1	7.7935	27452.6908
O95427	GPI ethanolamine phosphate transferase 1	3	2	15.032	104343.294
Q8WYB5	Histone acetyltransferase KAT6B	5	3	22.4955	234286.894
Q4VNC1	Probable cation-transporting ATPase 13A4	2	1	9.1325	135811.769
A0A494C073	Dystonin (Fragment)	6	3	22.5141	153503.768
P05129	Protein kinase C	3	2	15.7724	75634.0416
P06744	Glucose-6-phosphate isomerase (Fragment)	2	1	11.8535	31662.2129
P05155	Plasma protease C1 inhibitor	5	4	17.0378	55382.4019
Q8N4C6	Ninein	3	1	10.3272	240189.413
P00915	Carbonic anhydrase 1	4	2	17.9352	28927.2649
Q502W6	von Willebrand factor A domain-containing protein 3B	6	2	29.3765	147116.697
A2RTX5	Threonine–tRNA ligase 2_ cytoplasmic	3	2	12.5508	93672.2044
Q8IYD8	Fanconi anemia group M protein	4	1	22.2644	234986.16
Q8WXG6	MAP kinase-activating death domain protein	4	1	18.1507	184615.183
Q15646	2′-5′-oligoadenylate synthase-like protein	2	1	8.3398	42865.0201
A0A7I2V4E6	Zinc finger FYVE domain-containing protein 26 (Fragment)	2	1	8.894	98799.4852
Q7Z494	Nephrocystin-3	7	2	35.8915	152062.002
Q9ULX6	A-kinase anchor protein 8-like	2	1	14.3189	43353.9374
Q9NW75	G patch domain-containing protein 2	2	2	8.0253	59342.8597
Q9NQT8	Kinesin-like protein KIF13B	3	1	11.7525	204100.592
Q9H7U1	Serine-rich coiled-coil domain-containing protein 2	2	1	12.6581	94232.164
P0C0L4	Complement C4-A	19	2	113.6054	194382.511
Q92878	Zinc-hook domain-containing protein	3	2	16.6493	143854.181
P51648	Aldehyde dehydrogenase family 3 member A2 (Fragment)	3	2	19.4497	52276.7997
Q7L2Z9	Centromere protein Q	2	2	9.5498	30652.37
P08243	Asparagine synthetase [glutamine-hydrolyzing]	2	1	7.8618	46425.2272
Q9NQ36	Signal peptide_ CUB and EGF-like domain-containing protein 2	2	2	8.0104	117888.488
Q2TAK8	PWWP domain-containing DNA repair factor 3A	3	1	15.1654	79719.7991
O75376-3	Nuclear receptor corepressor 2 (Fragment)	2	1	9.0018	160852.457
A0A3B3ISJ8	CAP-Gly domain-containing linker protein 1 (Fragment)	6	1	30.3825	100093.39
Q6UWU2	Beta-galactosidase-1-like protein	2	1	9.0557	74443.3449
O95235	Kinesin-like protein KIF20A	9	1	44.7432	101304.596
O76090	Bestrophin OS=*Homo sapiens*	2	1	9.0242	51057.3443
Q08378	Golgin subfamily A member 3	6	1	31.5112	167868.182
Q6ZP82	Coiled-coil domain-containing protein 141	3	1	13.5496	167288.014
A5YKK6-3	Isoform 3 of CCR4-NOT transcription complex subunit 1	5	1	17.9421	243370.847
Q14667-3	Isoform 3 of Protein KIAA0100	6	2	15.816	44753.3825
Q01518	Adenylyl cyclase-associated protein 1	2	2	7.0146	52357.7623
Q5JRA6	Transport and Golgi organization protein 1 homolog	5	1	18.5658	214387.025
O75369-4	Filamin-B	3	1	12.1226	244915.503
Q5TA45	Integrator complex subunit 11	3	1	11.4433	68404.0912
Q8WX92	Negative elongation factor B	2	1	10.9851	70666.4399
Q9Y6X9	ATPase MORC2	2	1	11.1575	118621.722
Q70EK8	Inactive ubiquitin carboxyl-terminal hydrolase 53	3	1	12.0216	122745.377
P05156	Uncharacterized protein	2	1	9.1063	74234.2988

(*continued on next page*)

Table 2 (*continued*)

Accession #	Description	Peptide count	Unique peptides	Confidence score	Mass
P06576	ATP synthase subunit beta_ mitochondrial	4	2	25.492	56560.0088
Q9NSK0	Kinesin light chain 4	5	1	21.4168	69095.8424
Q14112	Nidogen-2	4	1	15.6918	154048.247

*The confidence score is the sum of the scores of the individual peptides, the higher the better.

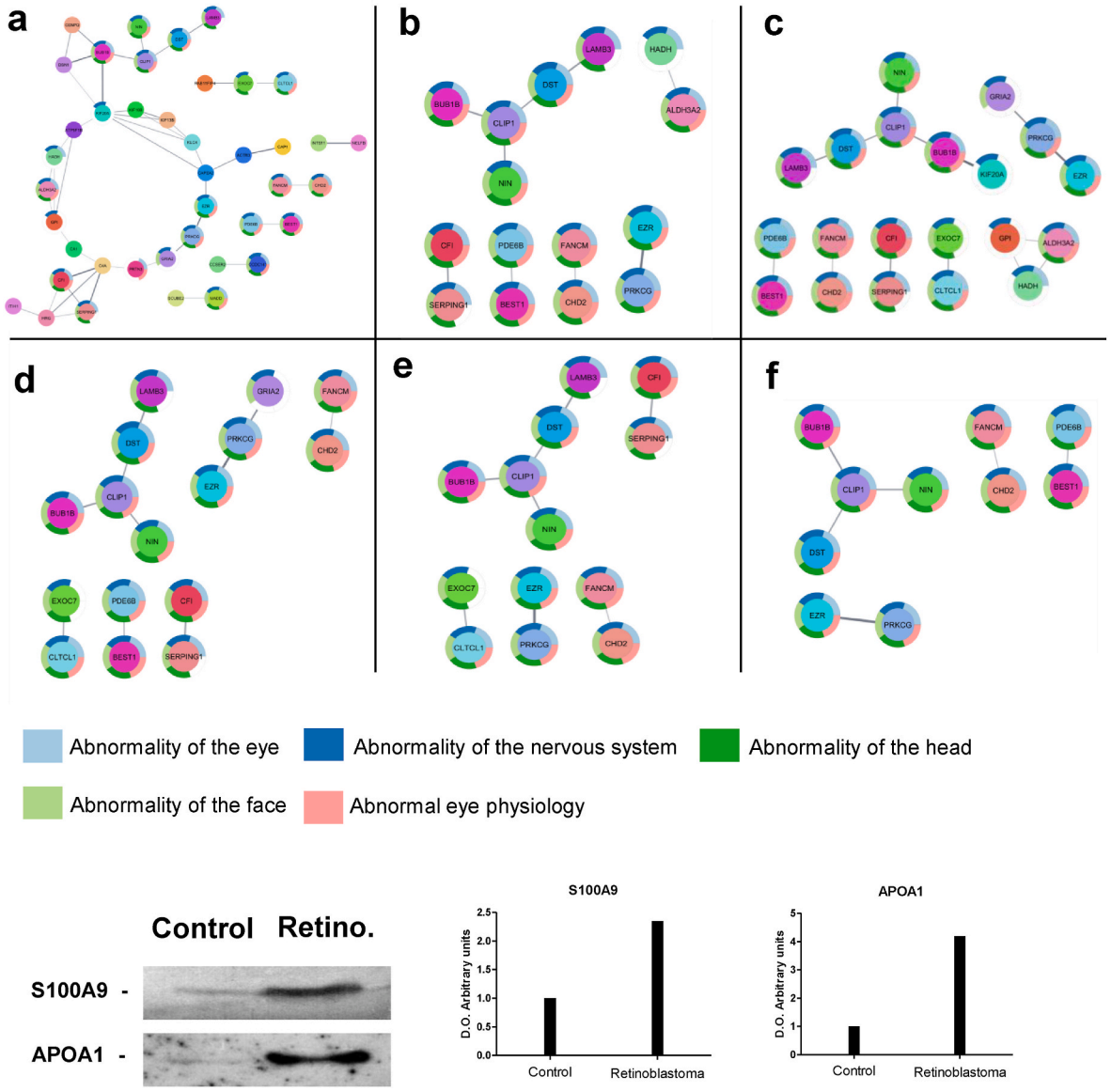

Fig. 2. Interaction networks of proteins present only in retinoblastoma condition. The network in (a) shows the interacting proteins according to monarch phenotype category which associates diseases and genotypes. Within this category the top 5 significant phenotypes with lowest FDR p-value are as follows (b) Abnormality of the eye, (c) Abnormality of the nervous system, (d) Abnormality of the head, (e) Abnormality of the face and (f) Abnormality of the eye physiology. Note that many proteins are involved in more than one molecular function, therefore each protein is encircled with color bars that indicate in which other process it is involved in. In the lower panel, the Western blot analysis of both S100A9 and APOA1 shows correlation with the mass spectrometry data (see Fig. 1 b). The loaded protein samples were aliquots identical to those analyzed by MS/MS. As expected, both are upregulated by more than two-fold.

Endothelial Growth Factor Receptor-2 (VEGFR2), and thus promoting vascular leakage and metastasis [36]. KIF16B promotes invasion as well but through the fast recycling of matrix metalloprotease MT1-MMP to the surface of macrophages [37].

Ezrin (EZR) is a common protein in every category in Fig. 2. This protein is recognized as a key player in adhesion process, thus it has crucial roles in invasion and metastasis in several cancers, presumably through activation of Focal Adhesion Kinase (FAK)/AKT signaling pathway [38]. Silencing EZR in lung adenocarcinoma cells led to apoptosis and the malignant phenotype was attenuated [39]. In accordance to our findings, EZR was proposed as a new biomarker in urine from patients with prostate cancer [40].

3.4. *Validation of proteomic data*

We proposed APOA1, S100A9, phosphatidylinositol 4-phosphate 5-

kinase (PIP5K) and Spliceosome Factor 3B (SF3B1) for their validation by Western blot; we chose these proteins because they exhibited high abundance with statistical significance. Unfortunately, we could not detect the las two proteins. However, the western blots of APOA1 and S100A9 showed an important difference between healthy controls and retinoblastoma patients (Fig. 2, lower panel). The normalized data to lactoferrin (LTF) shows more than two-fold higher the expression of both APOA1 and S100A9. Lactoferrin was chosen as a loading control because the proteomic analysis showed it had a less fold change between health and retinoblastoma condition (see LTF in Fig. 1 b).

4. Discussion

Since the beginning of the study of tears as biological material with diagnostic value in 1997 [41], many tear-based studies have been done on several diseases such as keratoconus, macular degeneration, dry-eye syndrome, thyroid eye disease, uveitis, Sjögren's syndrome, and even diabetes. These reports reveal a high complexity and probed utility providing information useful for the diagnosis and prognosis of several ocular and non-ocular diseases [7–10,42–51]. Yet, to the best of our knowledge this is the first approach for the search of non-invasive molecular markers by using tears in retinoblastoma patients.

There are few studies on Retinoblastoma through proteomic strategies. For instance, Mallikarjuna, through 2D-Electrophoresis gel identified 27 proteins in tumor tissue of retinoblastoma in comparison to health retina among 45-55 years old patients [52]; they found over expressed CRABP2, peroxiredoxin 6, apolipoprotein A1 and recoverin proteins in the retinoblastoma condition. In accordance, within our data we found up-regulated peroxiredoxin 2 and APOA1. Afterward, the same authors explored the proteomes of primary retinoblastoma tumors; again, as in our analysis, they observed the expression of APOA1 elevated in retinoblastoma tumors as well as peroxiredoxin 6, CRABP2, and recoverin [52]. APOA1 has been observed elevated in urine and serum in other cancers. Indeed, it was proposed as a potential biomarker for solid tumors [53].

Kinesin-like protein 11 (KIF11) is another protein that has been reported over expressed in retinoblastoma and is associated with late diagnosis [54]. KIF11 is a protein that is part of the 14-member kinesin family that participates in cell division, vesicular transport and organelles. Interestingly, we found its orthologue Kinesin-like protein 1A (KIF1A) overexpressed in the retinoblastoma condition. In other report, 431 proteins were identified in vitreous humor of patients with retinoblastoma using iTRAQ peptide labelling. Their major observations were the upregulation of proteins related to p38MAPK and Akt pathways, however we did not find coincidences within our data [55].

Another report that supports our findings, compared 4 different workflows for proteomic analysis of tear fluid using Schirmer method, only in healthy individuals. They achieved the identification of 3370 proteins, remarking 50 proteins that are the most abundant in the tear film [56]. Comparing our data with these results, we found coincidence with 21 proteins, among these, we observed 6 overexpressed in retinoblastoma condition (Actin cytoplasmic 2, Actin alpha skeletal muscle, Albumin, Pyruvate kinase PKM, Aldehyde dehydrogenase 1A1, Glutathione S-transferase P) and 4 under expressed (Cystatin- S, Extracellular glycoprotein lacritin, Lysozyme C and Prolactin-inducible protein).

It is also interesting the use of the tear in non-ocular diseases; for instance, the tear proteome of patients with chronic renal failure was compared with healthy subjects. In this study, 1139 proteins were screened, 77 and 135 were found up-and down-regulated, respectively [57]. Strikingly, APOA1, S100A8, and S100A9 were coincidently up-regulated as in our study. Another group searched for protein changes among young wearers of different types of contact lens. Although this group reported a huge number of proteins identified (3406), the most abundant proteins that they showed are not similar as in our findings [51].

It is important to note that the number of samples herein studied are still far from being sufficient to claim that we have identified a perfect array of bonafide biomarkers. To achieve this goal, it will take years testing every possible Mexican newborn, challenging the biomarkers for distinguish whether it is a real case or not of retinoblastoma. Nonetheless, it is encouraging that as evidenced in this discussion, some of the proteins we found altered either up- or downregulated, have also been reported in tissue of retinoblastoma or other malignancies, and some of them are even considered as potential biomarkers. This led us to think that our findings in tears are proteins that are truly altered in this silent disease.

5. Conclusion

As far as we know, there no exist any molecular biomarker for the early detection of retinoblastoma. Although other studies have explored retinoblastoma focusing on tumors or vitreous humor, this is the first approach intended to explore biomarkers through a non-invasive way. Next, these and other proposed biomarkers shall be tested in a broader number of patients in the following biomarker validation phases.

Ethics statement

The study was developed within the framework of the approved protocol number 12–17 by the committee of research and ethics from the Central Hospital "Ignacio Morones Prieto" San Luis Potosí, SLP, México. The ethics committee specifically approved this study. Diagnostic and therapeutic maneuvers were carried out according to the Official Mexican Standard NOM- 012-SSA3-2012, 2012 as well as with the current international codes for good practices in clinical research. The principles of the Helsinki Act of 1964 and its last revision in October 2013 were not transgressed. Written/signed informed consent was obtained from all the subject's parents in this study and the guardians on behalf of the minors involved in the study before samples were collected and clinical data were obtained from all subjects during the interview and clinical examination.

Funding

We thank to the Secretariat of Science, Humanities, Technology and Innovation (SECIHTI) for the grant CF-2023-338 and CBF2023-2024-2470.

Declaration of competing interest

The authors declare that they have no known competing financial interests or personal relationships that could have appeared to influence the work reported in this paper.

Acknowledgements

We are thankful for the technical support of Maria Luisa Labra Barrios. Mass spectrometry-based proteomics was performed in Genomics, Proteomics and Metabolomics Core Facility (UGPM), LaNSE, CINVESTAV-IPN; hence, we want to thank MSc. Emmanuel Ríos Castro and ChemE. Nataly Ramos Buendía for their help during LC-MS analysis and sample preparation respectively.

Appendix A. Supplementary data

Supplementary data to this article can be found online at https://doi.org/10.1016/j.jlb.2026.100471.

References

[1] Kivela T. The epidemiological challenge of the most frequent eye cancer: retinoblastoma, an issue of birth and death. Br J Ophthalmol 2009;93(9):1129–31.

[2] Howe HL, et al. Annual report to the nation on the status of cancer, 1975-2003, featuring cancer among U.S. Hispanic/Latino populations. Cancer 2006;107(8):1711–42.
[3] Garza-Garza LA, et al. Challenge of Retinoblastoma in Mexico in 2020: perspectives and solutions. J Ophthalmol 2020;2020:1953602.
[4] Goddard AG, Kingston JE, Hungerford JL. Delay in diagnosis of retinoblastoma: risk factors and treatment outcome. Br J Ophthalmol 1999;83(12):1320–3.
[5] Sarhadi VK, Armengol G. Molecular biomarkers in cancer. Biomolecules 2022;12(8).
[6] Zhan X, et al. Mass spectrometry analysis of human tear fluid biomarkers specific for ocular and systemic diseases in the context of 3P medicine. EPMA J 2021;12(4):449–75.
[7] Lepine M, Robert MC, Sleno L. Discovery and verification of Sjogren's Syndrome protein biomarkers in tears by targeted LC-MRM. J Proteome Res 2024;23(6):2219–29.
[8] Han JS, et al. Tear-derived exosome proteins are increased in patients with thyroid eye disease. Int J Mol Sci 2021;22(3).
[9] Maccora I, et al. Candidate tear-based uveitis biomarkers in children with JIA based on arthritis activity and topical corticosteroid use. Ocul Immunol Inflamm 2024:1–10.
[10] Angelopoulou E, et al. Tear proteomics in children and adolescents with type 1 diabetes: a promising approach to biomarker identification of diabetes pathogenesis and complications. Int J Mol Sci 2024;25(18).
[11] Martinez-Sanchez M, et al. Analysis of the p53 pathway in peripheral blood of retinoblastoma patients; potential biomarkers. PLoS One 2020;15(6):e0234337.
[12] Stevens S. Schirmer's test. Community Eye Health 2011;24(76):45.
[13] Rios-Castro E, et al. Quantitative proteomic analysis of MARC-145 cells infected with a Mexican porcine reproductive and respiratory syndrome virus strain using a label-free based DIA approach. J Am Soc Mass Spectrom 2020;31(6):1302–12.
[14] Azotla-Vilchis C, et al. Identification of dystrophin Dp71d(Delta71)-associated proteins in PC12 cells by quantitative proteomics. Biochim Biophys Acta Proteins Proteom 2024;1873(1):141049.
[15] Lou R, Shui W. Acquisition and analysis of DIA-based proteomic data: a comprehensive survey in 2023. Mol Cell Proteomics 2024;23(2):100712.
[16] Kall L, et al. Assigning significance to peptides identified by tandem mass spectrometry using decoy databases. J Proteome Res 2008;7(1):29–34.
[17] Elias JE, Gygi SP. Target-decoy search strategy for mass spectrometry-based proteomics. Methods Mol Biol 2010;604:55–71.
[18] Silva JC, et al. Absolute quantification of proteins by LCMSE: a virtue of parallel MS acquisition. Mol Cell Proteomics 2006;5(1):144–56.
[19] Barrera-Rojas J, et al. An initial proteomic analysis of biogas-related metabolism of euryarchaeota consortia in sediments from the Santiago River, Mexico. Microorganisms 2023;11(7).
[20] Szklarczyk D, et al. The STRING database in 2023: protein-protein association networks and functional enrichment analyses for any sequenced genome of interest. Nucleic Acids Res 2023;51(D1):D638–46.
[21] Coumans JVF, Davey RJ, Moens PDJ. Cofilin and profilin: partners in cancer aggressiveness. Biophys Rev 2018;10(5):1323–35.
[22] Cheng YJ, et al. Silencing profilin-1 inhibits gastric cancer progression via integrin beta1/focal adhesion kinase pathway modulation. World J Gastroenterol 2015;21(8):2323–35.
[23] Lu X, et al. Bioinformatics analysis of KIF1A expression and gene regulation network in ovarian carcinoma. Int J Gen Med 2021;14:3707–17.
[24] Danda R, et al. Proteomic profiling of retinoblastoma by high resolution mass spectrometry. Clin Proteom 2016;13:29.
[25] Khan MI, et al. Lysozyme as the anti-proliferative agent to block the interaction between S100A6 and the RAGE V domain. PLoS One 2019;14(5):e0216427.
[26] Mukohara T, et al. Inhibition of lysine acetyltransferase KAT6 in ER(+)HER2(-) metastatic breast cancer: a phase 1 trial. Nat Med 2024;30(8):2242–50.
[27] Meng D, et al. Glutamine and asparagine activate mTORC1 independently of Rag GTPases. J Biol Chem 2020;295(10):2890–9.
[28] Kim SH, et al. Mitochondrial Threonyl-tRNA synthetase TARS2 is required for threonine-sensitive mTORC1 activation. Mol Cell 2021;81(2):398–407 e4.
[29] Chen Y, et al. S100A8 and S100A9 in cancer. Biochim Biophys Acta Rev Cancer 2023;1878(3):188891.
[30] Jiang H, et al. Calcium-binding protein S100P and cancer: mechanisms and clinical relevance. J Cancer Res Clin Oncol 2012;138(1):1–9.
[31] Hao W, et al. S100P as a potential biomarker for immunosuppressive microenvironment in pancreatic cancer: a bioinformatics analysis and in vitro study. BMC Cancer 2023;23(1):997.
[32] Zeng Q, et al. Knockdown of BUB1B inhibits the proliferation, migration, and invasion of colorectal cancer by regulating the JNK/c-Jun signaling pathway. Cancer Biother Radiopharm 2024;39(3):236–46.
[33] Meng X, et al. KDELR2-KIF20A axis facilitates bladder cancer growth and metastasis by enhancing Golgi-mediated secretion. Biol Proced Online 2022;24(1):12.
[34] Xiong M, et al. KIF20A promotes cellular malignant behavior and enhances resistance to chemotherapy in colorectal cancer through regulation of the JAK/STAT3 signaling pathway. Aging (Albany NY) 2019;11(24):11905–21.
[35] Jin W, Ye L. KIF4A knockdown suppresses ovarian cancer cell proliferation and induces apoptosis by downregulating BUB1 expression. Mol Med Rep 2021;24(1).
[36] Waters SB, et al. KIF13B-mediated VEGFR2 trafficking is essential for vascular leakage and metastasis in vivo. Life Sci Alliance 2022;5(1).
[37] Hey S, et al. KIF16B drives MT1-MMP recycling in macrophages and promotes co-invasion of cancer cells. Life Sci Alliance 2023;6(11).
[38] Xu J, Zhang W. EZR promotes pancreatic cancer proliferation and metastasis by activating FAK/AKT signaling pathway. Cancer Cell Int 2021;21(1):521.
[39] Yu X, et al. Silencing lncRNA EZR-AS1 induces apoptosis and attenuates the malignant properties of lung adenocarcinoma cells. Acta Biochim Pol 2023;70(3):713–9.
[40] Vujicic I, et al. Potential role of seven proteomics tissue biomarkers for diagnosis and prognosis of prostate cancer in urine. Diagnostics 2022;12(12).
[41] Molloy MP, et al. Establishment of the human reflex tear two-dimensional polyacrylamide gel electrophoresis reference map: new proteins of potential diagnostic value. Electrophoresis 1997;18(15):2811–5.
[42] Zhou L, Beuerman RW. Tear analysis in ocular surface diseases. Prog Retin Eye Res 2012;31(6):527–50.
[43] Tiffany JM. Tears in health and disease. Eye (Lond) 2003;17(8):923–6.
[44] Lema I, et al. Proteomic analysis of the tear film in patients with keratoconus. Mol Vis 2010;16:2055–61.
[45] Winiarczyk M, et al. Tear film proteome in age-related macular degeneration. Graefes Arch Clin Exp Ophthalmol 2018;256(6):1127–39.
[46] Saijyothi AV, et al. Two dimensional electrophoretic analysis of human tears: collection method in dry eye syndrome. Electrophoresis 2010;31(20):3420–7.
[47] Gerber-Hollbach N, et al. Tear film proteomics reveal important differences between patients with and without ocular GvHD after allogeneic hematopoietic cell transplantation. Investig Ophthalmol Vis Sci 2018;59(8):3521–30.
[48] Aluru SV, et al. Tear fluid protein changes in dry eye syndrome associated with rheumatoid arthritis: a proteomic approach. Ocul Surf 2017;15(1):112–29.
[49] Zhou L, et al. In-depth analysis of the human tear proteome. J Proteonomics 2012;75(13):3877–85.
[50] Green-Church KB, et al. Investigation of the human tear film proteome using multiple proteomic approaches. Mol Vis 2008;14:456–70.
[51] Qin G, et al. Tear proteomic analysis of young glasses, orthokeratology, and soft contact lens wearers. J Proteonomics 2023;270:104738.
[52] Mallikarjuna K, et al. Comparative proteomic analysis of differentially expressed proteins in primary retinoblastoma tumors. Proteonomics Clin Appl 2010;4(4):449–63.
[53] Aalami AH, Aalami F, Sahebkar A. Apolipoprotein A-1 as a potential biomarker for solid tumors: a systematic review and meta-analysis. Curr Med Chem 2023;30(29):3356–67.
[54] Madhavan J, et al. High expression of KIF14 in retinoblastoma: association with older age at diagnosis. Investig Ophthalmol Vis Sci 2007;48(11):4901–6.
[55] Naru J, et al. Proteomic analysis of differentially expressed proteins in vitreous humor of patients with retinoblastoma using iTRAQ-coupled ESI-MS/MS approach. Tumour Biol 2016;37(10):13915–26.
[56] Jones G, et al. Comparison of different mass spectrometry workflows for the proteomic analysis of tear fluid. Int J Mol Sci 2022;23(4).
[57] Zong RR, et al. Tear dynamics testing and quantitative proteomics analysis in patients with chronic renal failure. J Proteonomics 2021;248:104351.